Thermophoretic Deposition of Nanoparticles Due To a Permeable Rotating Disk: Effects of Partial Slip, Magnetic Field, Thermal Radiation, Thermal-Diffusion, and Diffusion-Thermo

M. M. Rahman

Abstract—The present contribution deals with the thermophoretic deposition of nanoparticles over a rapidly rotating permeable disk in the presence of partial slip, magnetic field, thermal radiation, thermal-diffusion, and diffusion-thermo effects. The governing nonlinear partial differential equations such as continuity, momentum, energy and concentration are transformed into nonlinear ordinary differential equations using similarity analysis, and the solutions are obtained through the very efficient computer algebra software MATLAB. Graphical results for non-dimensional concentration and temperature profiles including thermophoretic deposition velocity and Stanton number (thermophoretic deposition flux) in tabular forms are presented for a range of values of the parameters characterizing the flow field. It is observed that slip mechanism, thermal-diffusion, diffusion-thermo, magnetic field and radiation significantly control the thermophoretic particles deposition rate. The obtained results may be useful to many industrial and engineering applications.

Keywords—Boundary layer flows, convection, diffusion-thermo, rotating disk, thermal-diffusion, thermophoresis.

NOMENCLATURE

B_0	magnetic induction [Wb.m^{-1}]
C	species concentration in the boundary layer [kg.m^{-3}]
C_m, C_s, C_t	constants in (9)
C_1, C_2, C_3	constants in (9)
C_∞	species concentration of the ambient fluid [kg.m^{-3}]
c_p	specific heat at constant pressure
D_m	diffusion coefficient [m^2.s^{-1}]
Df	Soret number
Du	Dufour number
d_p	particle diameter [m]
F	dimensionless radial velocity
G	dimensionless tangential velocity
H	dimensionless axial velocity
Ha	Hartmann number
J_w	rate of transfer of species concentration [kg.m^{-2}.s^{-1}]
Kn	Knudsen number
N_t	temperature parameter
p	pressure within the boundary layer [Pa]
p_∞	pressure outside the boundary layer [Pa]
P	nondimensional pressure
Pr	Prandtl number
q_r	radiative heat flux
R	conduction radiation parameter
Re_r	local Reynolds number
Sc	Schmidt number
St_r	local Stanton number
T	temperature of the fluid within the boundary layer [K]
T_m	mean temperature [K]
T_∞	temperature of the ambient fluid [K]
T_w	temperature at the surface of the disk [K]
u, v, w	r, θ, and z - components of the velocity field [m.s^{-1}]
U_∞	free stream velocity [m.s^{-1}]
U_T	thermophoretic velocity along radial direction [m.s^{-1}]
V_d	thermophoretic deposition velocity [m.s^{-1}]
V_d^*	nondimensional thermophoretic deposition velocity
W_T	thermophoretic velocity along axial direction [m.s^{-1}]
W_T^*	nondimensional thermophoretic velocity along axial direction
w_0	suction velocity [m.s^{-1}]
w_s	non-dimensional suction/injection velocity

Greek symbols

α	thermal diffusivity [m^2.s^{-1}]
ρ	fluid density [kg.m^{-3}]
κ	thermophoretic coefficient

M. M. Rahman is with the Department of Mathematics and Statistics, College of Science, Sultan Qaboos University, P.O. Box 36, Al-Khod 123, Muscat, Sultanate of Oman (Correspondence: phone: +968-2414-1423; fax: +968-2414-1490;e-mail: mansurdu @ yahoo.com, mansur@squ.edu.om).

World Academy of Science, Engineering and Technology
International Journal of Mathematical and Computational Sciences
Vol:7, No:5, 2013

k_1	mean absorption coefficient
η	similarity variable
ξ	target momentum accommodation coefficient
υ	kinematic viscosity [m^2.s^{-1}]
μ	fluid viscosity [Pa.s]
θ	dimensionless temperature
ϕ	dimensionless concentration
λ	mean free path [m]
σ	magnetic permeability
σ_1	Stefan-Boltzmann constant
λ_g	thermal conductivity of fluid [W.m^{-1}.K^{-1}]
λ_p	thermal conductivity of diffused particles [W.m^{-1}.K^{-1}]
Ω	angular velocity [s^{-1}]
Δ	increment
ε	slip factor
w	surface conditions
∞	Free stream conditions

I. INTRODUCTION

A radiometric force by temperature gradient that enhances small micron sized particles moving toward a cold surface and away from the hot surface is termed as thermophoresis. The velocity caused by thermophoresis is called thermophoretic velocity. Thermophoresis plays a significant role of transporting particles from hot fluid region to the cold fluid region. This phenomenon has many engineering applications in removing small particles from gas streams, in determining exhaust gas particle trajectories from combustion devices, and in studying the particulate material deposition on turbine blades. Thermophoresis principle is utilized to manufacture graded index silicon dioxide and germanium dioxide in the fabrication of optical fiber used in the field of communications. Thermophoresis is also a key mechanism of study in semi-conductor technology especially in production of controlled high-quality wafer as well as in production of magnetohydrodynamic (MHD) energy. Thermophoretic deposition of radioactive particles is one of the major factors causing accidents in nuclear reactors.

Radiative heat transfer is very important in manufacturing industries for the design of reliable equipment, nuclear power plants, gas turbines, and various propulsion devices for aircraft, missiles, satellites, and space vehicles. The effect of thermal radiation on the convective flows is also important in the context of space technology and processes involving high temperatures.

Due to the engineering and industrial applications of thermophoresis phenomenon many researchers (see for examples [1]-[12] and references there in) have studied and reported results on this topic considering various flow, heat and mass transfer conditions in different geometries. The general conclusion of these studies shows that a cold wall surface will lead to an increase of particle deposition due to thermophoresis. References [13]-[14] studied the effect of thermophoretic force in free convection boundary layer from a vertical flat plate embedded in a porous medium with heat generation or absorption. Reference [15] analyzed mixed convection flow, heat, and mass transfer over an isothermal vertical flat plate embedded in a fluid-saturated porous medium considering viscous dissipation and thermophoresis in both the cases of aiding and opposing flows. Reference [16] investigated the thermophoretic particle deposition on the free convection problem over a horizontal flat plate embedded in a fluid-saturated porous medium. In a series of papers [17]-[20], Alam et al. studied two-dimensional steady heat and mass transfer flow over an inclined flat plate with various flow conditions in the presence of thermophoresis. Reference [21] studied heat and mass transfer of thermophoretic magnetohydrodynamic flow over an inclined radiate isothermal permeable surface in the presence of heat source/sink.

They noticed that higher value of thermophoretic parameter contributes to lower fluid concentration. Very recently, [22] focused on the analysis of heat and mass transfer in boundary-layer free convection over an inclined flat plate embedded in a fluid saturated porous medium in the presence of thermophoresis. The significance of thermophoresis on the particles deposition was analyzed for both cold and hot wall cases.

The flow dynamics due to a rotating disk, early formulated by von Karman [23] is a popular area of research. Many researchers (see for examples, [24]-[31] and the references there in) have studied and reported results on disk-shaped bodies with or without heat transfer considering various flow conditions as they encountered in many industrial, geothermal, geophysical, technological and engineering applications few of them are rotating heat exchangers, rotating disk reactors for bio-fuels production, computer disk drives, gas or marine turbine. Reference [32] studied thermal-diffusion and diffusion-thermo effects on combined heat and mass transfer of a steady MHD convective and slip flow due to a rotating disk with viscous dissipation and Ohmic heating. Reference [33] studied convective hydromagnetic slip flow with variable properties due to a porous rotating disk.

Reference [34] studied particle deposition on a rotating disk in application to vapor axial deposition process. Deposition of the particles on the disk was examined, considering convection, diffusion, thermophoresis, and coagulation with variations of the forced flow velocity and the disk rotating velocity. They found that the deposition rate and the deposition efficiency directly increase as the flow velocity increases, resulting from that the increase of the forced flow velocity causes thinner thermal and diffusion boundary layer thicknesses and, thus, causes the increase of thermophoretic drift and Brownian diffusion of the particles toward the disk. Reference [35] investigated the combined effects of inertia, diffusion and thermophoresis on aerosol particle deposition from a stagnation point flow onto an axisymmetric wavy wafer. The numerical result of [35] revealed that the deposition effect was greatly controlled by the geometric shapes of the deposition surface and had a frequency similar to

World Academy of Science, Engineering and Technology
International Journal of Mathematical and Computational Sciences
Vol:7, No:5, 2013

that of surface geometry. Reference [36] studied combined effects of thermophoresis and electrophoresis on particle deposition on to a wavy surface disk including Brownian diffusion, convection and sedimentation. They found that for small particle, diffusion and thermophoresis are the major deposition mechanisms. Reference [37] studied thermophoretic deposition of particles due to a rotating disk. They found that axial particle deposition velocity increases as the thermophoretic coefficient as well as Schmidt number increases.

To the best of the author's knowledge no research about thermophoretic deposition of nanoparticles over a rapidly rotating permeable disk in the presence of partial slip considering the effects of thermal-diffusion, diffusion-thermo, magnetic field, and radiation was conducted. Therefore, in the present paper we take a forward step extending the work of [37] to investigate the thermophoretic deposition mechanism of nano particles on a cold rapidly rotating permeable disk with partial slip at its surface considering the effects of thermal-diffusion, diffusion-thermo, transverse magnetic field, and surface radiation. The resulting coupled nonlinear governing equations are solved for similarity solutions numerically using computer algebra software MATLAB. Graphical results for non-dimensional concentration and temperature profiles including thermophoretic deposition velocity and Stanton number (thermophoretic deposition flux) in tabular form are presented for a range of values of the parameters characterizing the flow field. The accompanying discussion provides physical interpretations of the results.

II. FORMULATION OF THE PROBLEM

A. Flow Analysis

In a non-rotating cylindrical polar frame of reference (r, ϕ, z), where z is the vertical axis in the cylindrical coordinates system with r and ϕ as the radial and tangential axes respectively, let us consider a disk which rotates with constant angular velocity Ω about the z-axis. The disk is placed at $z = 0$, and a viscous incompressible electrically conducting Newtonian fluid occupies the region $z > 0$. A magnetic field of uniform strength B_0 is applied along the direction normal to the surface of the disk. The flow configurations and geometrical coordinates are shown in Fig. 1.
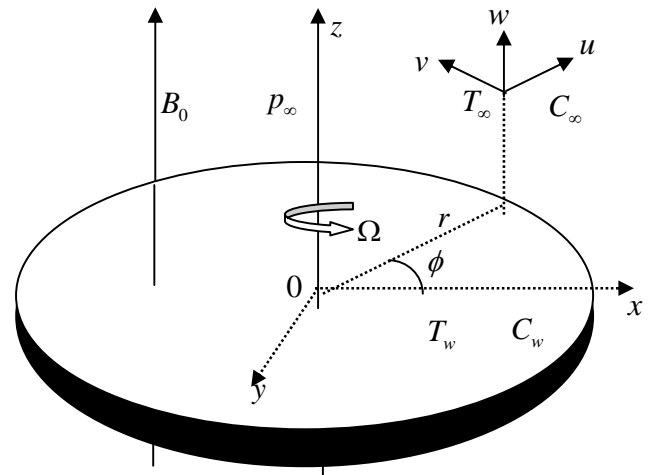

Fig. 1 Flow configurations and coordinate system

The components of the flow velocity $\mathbf{q}$ are (u, v, w) in the directions of increasing (r, ϕ, z) respectively. The surface of the rotating disk is maintained at a uniform temperature T_w and far away from the wall, the free stream temperature is $T_\infty (> T_w)$ and the pressure is p_∞. The species concentration at the surface is maintained uniform at C_w, which is taken to be zero and that of the ambient fluid is assumed to be C_∞. The effects of thermophoresis are being taken into account to help in the understanding of the mass deposition variation on the surface. We further assume that

(i)   the mass flux of particles is sufficiently small so that the main stream velocity and temperature fields are not affected by the thermo physical processes experienced by the relatively small number of particles,

(ii) when particles hit the disk surface, they will be absorbed by it and none will be bounced back,

(iii) due to the boundary layer behavior the temperature gradient in the z-direction is much larger than that in the r-direction and hence only the thermophoretic velocity component which is normal to the surface is of importance,

(iv) the fluid has constant kinematic viscosity and thermal conductivity,

(v)   the particle diffusivity is assumed to be constant, and the concentration of particles is sufficiently dilute to assume that particle coagulation in the boundary layer is negligible,

(vi) the flow is steady and axially symmetric,

(vii) The fluid is considered to be gray; absorbing-emitting radiation but non-scattering medium and the Rosseland approximation is used to describe the radiative heat flux in the energy equation. The radiative heat flux in the r, and θ-directions are considered negligible in comparison to the z-direction.

World Academy of Science, Engineering and Technology
International Journal of Mathematical and Computational Sciences
Vol:7, No:5, 2013

Under the afore-mentioned assumptions, the mass, momentum, energy and particle concentration equations become (see [32], [37]):

$$\frac{\partial u}{\partial r} + \frac{u}{r} + \frac{\partial w}{\partial z} = 0 , \tag{1}$$

$$u\frac{\partial u}{\partial r} - \frac{v^2}{r} + w\frac{\partial u}{\partial z} = -\frac{1}{\rho}\frac{\partial p}{\partial r} + \upsilon\left(\nabla^2 u - \frac{u}{r^2}\right) - \frac{\sigma B_0^2 u}{\rho} \tag{2}$$

$$u\frac{\partial v}{\partial r} + \frac{uv}{r} + w\frac{\partial v}{\partial z} = \upsilon\left(\nabla^2 v - \frac{v}{r^2}\right) - \frac{\sigma B_0^2 v}{\rho} \tag{3}$$

$$u\frac{\partial w}{\partial r} + w\frac{\partial w}{\partial z} = -\frac{1}{\rho}\frac{\partial p}{\partial z} + \upsilon\nabla^2 w \tag{4}$$

$$u\frac{\partial T}{\partial r} + w\frac{\partial T}{\partial z} = \alpha\nabla^2 T + \frac{D_m \lambda_g}{C_s c_p}\nabla^2 C - \frac{1}{\rho c_p}\frac{\partial q_r}{\partial z} \tag{5}$$

$$u\frac{\partial C}{\partial r} + w\frac{\partial C}{\partial z} = D_m\nabla^2 C - \frac{\partial}{\partial z}(W_T C) + \frac{D_m \lambda_g}{T_m}\nabla^2 T \tag{6}$$

where u, v, w are the velocity components in the r, θ and z directions respectively, υ isthe kinematic viscosity, p is the pressure, $\rho$is the density of the fluid, σ is the magnetic permeability, T, T_w, and T_∞ are the temperature of the fluid inside the thermal boundary layer, the disk temperature and the fluid temperature in the free stream, respectively, while C, C_w and C_∞ are the corresponding concentrations, λ_g is the thermal conductivity of the fluid, D_m is the diffusion coefficient, T_m mean temperature, W_T is the thermophoretic velocity along axial direction, and $\nabla^2 = \frac{\partial^2}{\partial r^2} + \frac{1}{r}\frac{\partial}{\partial r} + \frac{\partial^2}{\partial z^2}$ is the Laplacian operator.

The radiative heat flux q_r under Rosseland approximation has the form

$$q_r = -\frac{4\sigma_1}{3k_1}\frac{\partial T^4}{\partial z} \tag{7}$$

where σ_1 is the Stefan-Boltzmann constant and k_1 is the mean absorption coefficient.

The thermophoretic velocity W_T which appear in (6) recommended by [2] is defined as

$$W_T = -\frac{\kappa\upsilon}{T}\frac{\partial T}{\partial z} \tag{8}$$

where $\kappa\upsilon$ represents the thermophoretic diffusivity, and κ is the thermophoretic coefficient whose values range from 0.2 to 1.2 as indicated by [6] and is defined from the theory of [2] by

$$\kappa = \frac{2C_s(\lambda_g / \lambda_p + C_t Kn)[1 + Kn(C_1 + C_2 e^{-C_3/Kn})]}{(1+3C_m Kn)(1+2\lambda_g / \lambda_p + 2C_t Kn)} \tag{9}$$

where $C_1 = 1.2$, $C_2 = 0.41$, $C_3 = 0.88$, $C_m = 1.146$, $C_s = 1.147$, $C_t = 2.20$ are constants, λ_g and λ_p are the thermal conductivities of the fluid and diffused particles, respectively and $Kn = 2\lambda / d_p$ the Knudsen number, is the ratio of mean free path of gas molecules to particle diameter.

If mean free path of the fluid particles is comparable to the characteristic dimensions of the flow field domain the assumption of continuum media no longer valid as a consequence Navier–Stokes equation breaks down. In the range $0.1 < Kn < 10$ of Knudsen number, the high order continuum equations (Burnett equations) should be used. For the range of $0.001 < Kn < 0.1$, no-slip boundary conditions cannot be used and should be replaced with the following expression ([38]):

$$U_t = \lambda[(2-\xi)/\xi]\frac{\partial u}{\partial z} \tag{10}$$

where U_t is the target velocity, ξ is the target momentum accommodation coefficient and λ is the mean free path. For $Kn < 0.001$, the no-slip boundary condition is valid; therefore, the velocity at the surface is equal to zero.

B. Boundary Conditions

The applicable boundary conditions for the present model are

(i) on the surface of the disk($z = 0$):

$$u = U_t , \; v = \Omega r + U_t \text{ (slip flow)}$$
$$w = w_0 \text{ (permeable surface)}$$
$$T = T_w \text{ (uniform surface temperature)}$$
$$C = C_w = 0 \text{ (clean and fully absorbing surface).}$$
$$\tag{11}$$

(ii) matching with the quiescent free stream ($z \to \infty$):

World Academy of Science, Engineering and Technology
International Journal of Mathematical and Computational Sciences
Vol:7, No:5, 2013

$$u = 0, \; v = 0, \; T = T_\infty, \; C = C_\infty, \; p = p_\infty, \quad (12)$$

where the subscript w refer to the condition at the wall.

C. Introduction of Dimensionless Variables

To obtain the solutions of the governing (1)-(6) together with the boundary conditions (11)-(12) we introduce a dimensionless normal distance from the disk, $\eta = z(\Omega/\upsilon)^{1/2}$ along with the von-Karman transformations

$$\left.\begin{array}{l} u = \Omega r F(\eta), v = \Omega r G(\eta), w = (\Omega \upsilon)^{1/2} H(\eta), \\ p - p_\infty = \rho \upsilon \Omega P(\eta), T_\infty - T = \Delta T \theta(\eta), C = C_\infty \phi \end{array}\right\} \quad (13)$$

where υ_∞ is the kinematic viscosity of the ambient fluid and

$$\Delta T = T_\infty - T_w.$$

Now substituting (7) and (13) into (1)-(6) we obtain the following nonlinear ordinary differential equations

$$H' + 2F = 0 \quad (14)$$

$$F'' - HF' - F^2 + G^2 - Ha^2 F = 0 \quad (15)$$

$$G'' - HG' - 2FG - Ha^2 G = 0 \quad (16)$$

$$P' - H'' + HH' = 0 \quad (17)$$

$$\theta''\left[1 + \frac{4}{3R}(1 - N_t \theta)^3\right] - \frac{4N_t}{R}\theta'^2 (1 - N_t \theta)^2 - \Pr H\theta' - \Pr Du\phi'' = 0 \quad (18)$$

$$\phi'' - \left[\kappa ScN_t \frac{\theta'}{1 - N_t \theta} + ScH\right]\phi' - \kappa ScN_t \left[\frac{\theta''}{1 - N_t \theta} + \frac{N_t \theta'^2}{(1 - N_t \theta)^2}\right]\phi - ScDf\theta'' = 0 \quad (19)$$

where $\Pr = \upsilon/\alpha$ is the Prandtl number, $Sc = \upsilon/D_m$ is the Schmidt number, $Ha = B_0(\sigma/\rho\Omega)^{1/2}$ is the Hartmann number, $R = \lambda_g k_1 / 4\sigma T_\infty^3$ is the conduction-radiation parameter, $Df = D_m \lambda_g \Delta T / T_m \upsilon C_\infty$ is the thermal-diffusion (or Soret number) parameter, $Du = D_m \lambda_g C_\infty / C_s c_p \upsilon \Delta T$ is the diffusion-thermo (or Dufour number) parameter, $N_t = \Delta T / T_\infty$ is the temperature parameter, which is positive for a cooled surface and negative for a heated surface. In gases, $N_t > 0$ is associated with the

deposition of particles on the wall, while $N_t < 0$ may be thought as a mean to suppress the particle deposition, see for instance [39] for internal flows.

Thus by using (13) boundary conditions (11)-(12) become

$$F = \varepsilon F', G = 1 + \varepsilon G', H = w_s, \theta = 1, \phi = 0 \; \text{ at } \eta = 0 \quad (20)$$

$$F = 0, G = 0, P = 0, \theta = 0, \phi = 1 \; \text{ as } \eta \to \infty \quad (21)$$

where $\varepsilon = \lambda[(2 - \xi)/\xi](\Omega/\upsilon_\infty)^{1/2}$ is the slip parameter and $w_s = w_0(\Omega\upsilon)^{-1/2}$ represents a uniform suction when $w_s < 0$ and uniform injection when $w_s > 0$ at the surface of the disk.

D. Thermophoretic Velocity, Thermophoretic Particle Deposition Velocity, and Stanton Number

The quantities of engineering interest are the thermophoretic velocity, the thermophoretic particle deposition velocity, and the Stanton number. Thermophoretic velocities at the surface of the disk along radial and axial directions are evaluated as:

$$U_T]_{z=0} = 0$$

$$W_T]_{z=0} = -\frac{\kappa\upsilon}{T}\frac{\partial T}{\partial z}\bigg]_{z=0} = -\frac{\kappa N_t}{1 - N_t}\theta'(0)\sqrt{\Omega\upsilon} \quad (22)$$

A non-dimensional axial thermophoretic velocity can be introduced in the form:

$$W_T^* = W_T / \sqrt{\Omega\upsilon} = [\kappa N_t / (N_t - 1)]\theta'(0) \quad (23)$$

Thermophoretic particle deposition velocity at the surface of the disk is evaluated by

$$V_d = J_w / C_\infty]_{z=0} = -(1/Sc)\phi'(0)\sqrt{\Omega\upsilon} \quad (24)$$

where $J_w = -D\frac{\partial C}{\partial z}\bigg]_{z=0} = -\frac{D}{\upsilon}\phi'(0)\sqrt{\Omega\upsilon}C_\infty$ is the rate of transfer of species concentration.

Non-dimensional thermophoretic particle deposition velocity,

$$V_d^* = V_d / \sqrt{\Omega\upsilon} = -(1/Sc)\phi'(0) \quad (25)$$

The negative sign in (23) represents that particle deposition will take place at the surface of the disk from the hotter region to the colder region i.e. from the fluid to the disk along the inward axial direction.

World Academy of Science, Engineering and Technology
International Journal of Mathematical and Computational Sciences
Vol:7, No:5, 2013

The local Stanton number St_r is defined as

$$St_r = -J_w / C_\infty \Omega r = (1/Sc)\phi'(0) \mathrm{Re}_r^{-1/2} \qquad (26)$$

where $\mathrm{Re}_r = \Omega r^2 / \upsilon$.

$$\text{i.e. } St_r \mathrm{Re}_r^{1/2} = (1/Sc)\phi'(0) \qquad (27)$$

Now comparing (25) and (27) we find that

$$St_r \mathrm{Re}_r^{1/2} = -V_d^* \qquad (28)$$

Thus from (23), (25) and (27) we see that thermophoretic velocity is proportional to the numerical values of $-\theta'(0)$ whereas thermophoretic deposition velocity and Stanton number are proportional to $\phi'(0)$ which are evaluated when the corresponding differential equations are solved satisfying the convergence criteria.

III. NUMERICAL SOLUTIONS

The set of (14)-(19) are highly nonlinear and coupled and therefore it cannot be solved analytically. We dropped (17) from the system as it can be used for calculating pressure once H is known from the rest of the equations. The transformed governing (14)-(16) and (18)-(19) with boundary conditions (20)-(21) are solved numerically using the very robust computer algebra software MATLAB. The software is well tested and has been successfully used (see [40]) to study a variety of nonlinear heat, mass and fluid flow problems.

IV. NUMERICAL EXPERIMENT

Here, we investigate thermophoretic deposition of particles due to the three dimensional steady forced convective hydromagnetic laminar flow of a viscous incompressible fluid over a rapidly rotating porous disk in the presence of partial slip at its surface. The effects of thermal-diffusion and diffusion-thermo on the particle deposition mechanism together with the effect of thermal radiation are also taken into account. It can be seen that the numerical solutions are affected by the Hartmann number Ha, radiation parameter R, thermophoretic coefficient κ, temperature parameter N_t, suction (or injection) parameter w_s, thermal-diffusion parameter Df, diffusion-thermo parameter Du, slip parameter ε, Prandtl number Pr, and Schmidt number Sc. Since experimental data of the physical parameters are not available therefore in the numerical simulations the choice of the values of the parameters was dictated by the values chosen by the previous investigators.

For the present investigation we considered our working fluid as air ($\mathrm{Pr} = 0.71$). The default values of the other parameters are considered to be $Ha = 0.5$, $R = 1.0$, $w_s = -1.0$, $\varepsilon = 0.2$, $Df = 0.2$, $Du = 0.3$, $N_t = 0.1$, $Sc = 10$, and $\kappa = 0.5$ unless otherwise specified.

A. Code Verification

For $Ha = 0$, $w_s = 0$, $R \to \infty$, $Df = 0$, $Du = 0$, and $\varepsilon = 0$ the present problem coincides exactly with that of [37]. To assess the accuracy of the present code, we reproduced the values of the Stanton number ($St_r \mathrm{Re}_r^{1/2} = -V_d^*$) for different values of κ, Sc, and N_t for $Ha = 0$, $w_s = 0$, $R \to \infty$, $Df = 0$, $Du = 0$, $\varepsilon = 0$ and $\mathrm{Pr} = 0.71$. Tables I and II show the comparisons of the data produced by the present code and that of [37]. We found excellent agreement among the data. Further in the absence of mass transfer and for $\kappa = 0$, $N_t = 0$, $Df = 0$, $Du = 0$, $w_s = 0$, $Ha = 0$, $\varepsilon = 0$, and $R \to \infty$ the present model also coincides with that of [24] . Thus, we reproduced the values of $F'(0)$, $-G'(0)$ and $-\theta'(0)$ for $\mathrm{Pr} = 0.71$ and presented in Table III. In fact these results show an excellent agreement, hence justify the use of the present code for the current model.

TABLE I
VARIATIONS OF STANTON NUMBER $St_r \mathrm{Re}_r^{1/2} (= -V_d^*)$ (OR INWARD AXIAL THERMOPHORETIC DEPOSITION VELOCITY) FOR DIFFERENT VALUES OF κ AT $\mathrm{Pr} = 0.71$, $Sc = 0.94$ AND $N_t = 0.5$

κ	0	0.5	0.8	1.2
Present	0.40743	0.42396	0.43345	0.44569
[37]	0.407432	0.423963	0.433450	0.445649

TABLE II
VARIATIONS OF STANTON NUMBER $St_r \mathrm{Re}_r^{1/2} (= -V_d^*)$ (OR INWARD AXIAL THERMOPHORETIC DEPOSITION VELOCITY) FOR DIFFERENT VALUES OF Sc AT $\mathrm{Pr} = 0.71$, $\kappa = 0.5$ AND $N_t = 0.1$

Sc	0.22	0.60	0.94	2000
Present	0.67086	0.49300	0.40993	0.01791
[37]	0.670863	0.493005	0.409938	0.017916

TABLE III
NUMERICAL VALUES OF $F'(0)$, $-G'(0)$ AND $-\theta'(0)$ FOR $\mathrm{Pr} = 0.71$, $Sc = \kappa = N_t = Df = Du = w_s = Ha = 0$, $R \to \infty$ AND FOR NO MASS TRANSFER

	$F'(0)$	$-G'(0)$	$-\theta'(0)$
Present	0.510223	0.615923	0.325866
[24]	0.510233	0.615922	0.325856

V. RESULTS AND DISCUSSION

The numerical results are presented in the form of non-dimensional concentration and temperature profiles for various values of the pertinent parameters. Parametric studies are conducted by varying the Hartmann number Ha,

World Academy of Science, Engineering and Technology
International Journal of Mathematical and Computational Sciences
Vol:7, No:5, 2013

radiation parameter R, suction (or injection) parameter w_s, slip parameter ε, Soret number Df, Dufour number Du, temperature parameter N_t, Schmidt number Sc, and thermophoretic coefficient κ. Following the definition of the temperature parameter it can be found that $N_t < 1$ always. On the other hand, we restrict ourselves to the case of a cold wall ($T_w < T_\infty$), which means N_t should be positive.

To investigate the effect of the applied magnetic field on the thermophoretic deposition of particles we varied the Hartmann number within the flow domain as depicted in Fig. 2 (a). It can be noticed that the concentration of the particles decreases with the increase of the Hartmann number Ha. On the other hand the temperature of the fluid within the boundary layer increases with the increase of the Hartmann number as displayed in Fig. 2 (b). The applied magnetic field interacts with the flow field and creates Lorentz force which in turn decelerates the fluid velocity and enhances its temperature to rise. It can further be noted that the thicknesses of the concentration as well as thermal boundary layers increase with the increase of the strength of the applied magnetic field. Thus, a magnetic field can control the deposition of the particles on the disk surface in an expense of increasing the disk's surface temperature.
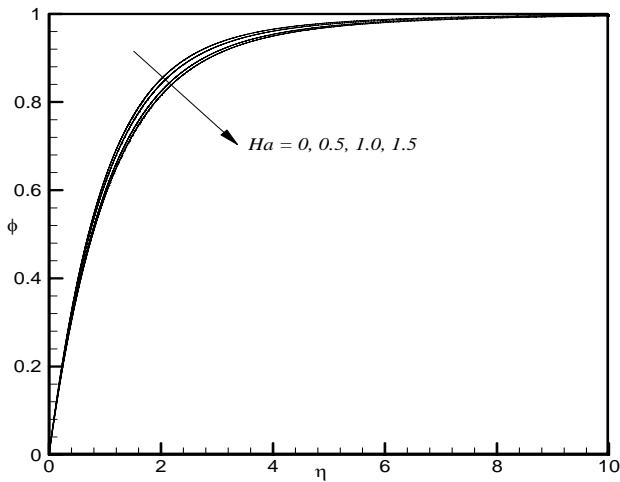

Fig. 2 (b) Temperature variation for different values of Ha
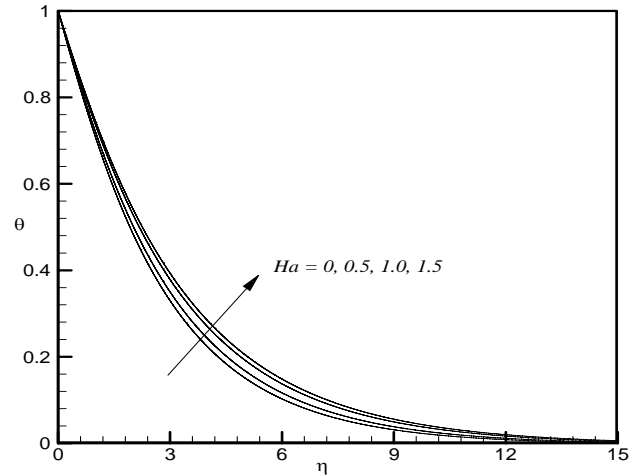

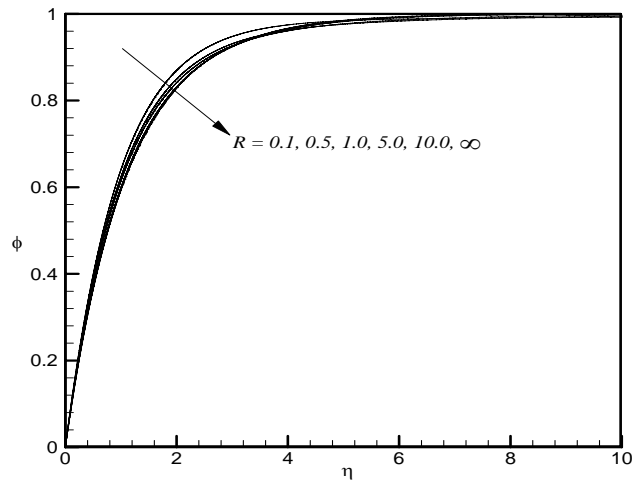Fig. 3 (a) Concentration variation for different values of R

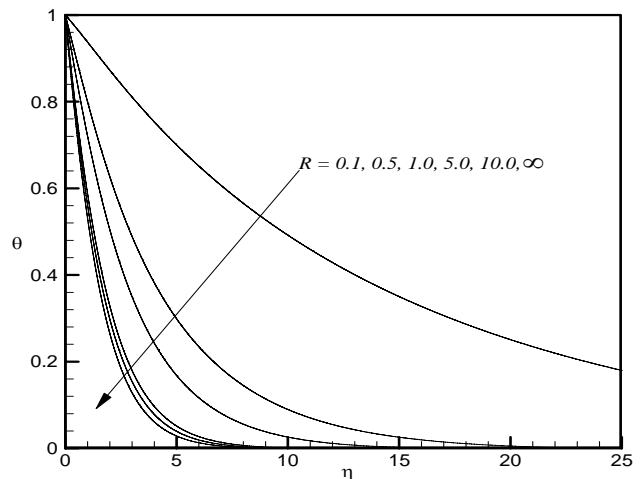Fig. 2 (a) Concentration variation for different values of Ha

Fig. 3 (b)Temperature variation for different values of R

Figs. 3 (a)-(b), respectively, shows the distribution of concentration and temperature profiles within the boundary layer for different values of the conduction-radiation

World Academy of Science, Engineering and Technology
International Journal of Mathematical and Computational Sciences
Vol:7, No:5, 2013

parameter R. From Fig. 3 (a) it is observed that the concentration profile decreases and the thickness of the concentration boundary layer increases with the increase of the conduction-radiation parameter. From Fig. 3 (b) it is found that the increasing of the conduction-radiation parameter increases temperature gradient near the surface of the disk, which increases heat transfer rates, this is due to the fact that the effect of radiation increases temperature of the flow field and the absence of radiation defines small temperatures.

Increasing suction causes a stronger adherence of the flow to the wall as a consequence boundary layer thickness reduced. This serves to decelerate the flow hence boundary layer can be controlled applying strong suction. In order to examine the effect of thermophoresis on the particle deposition onto a rotating disk surface, the concentration profiles against η are illustrated in Fig. 4 (a), for different values of the suction parameter w_s. Fig. 4 (a) shows that as suction ($w_s < 0$) intensifies concentration of particles across the boundary layer increases. Variation of nondimensional temperature profiles for various values of the suction parameter w_s is shown in Fig. 4 (b). An increase in suction clearly cools the boundary layer regime as a consequence temperature of the fluid fall rapidly with a rise in w_s from 0, -1, -2, and -3. With a greater suction the profiles also descend more rapidly from the peak surface temperature i.e. the distributions exhibit steeper negative gradients for stronger suction ($w_s = -3$) than for no suction ($w_s = 0$). Suction therefore acts as a powerful mechanism for cooling the flow and such features are important in high temperature energy systems such as magnetohydrodynamic power generators, nuclear energy processes etc. This figure also shows that thermal boundary layer thickness decreases with the increase of the suction velocity even in the presence of thermophoresis.
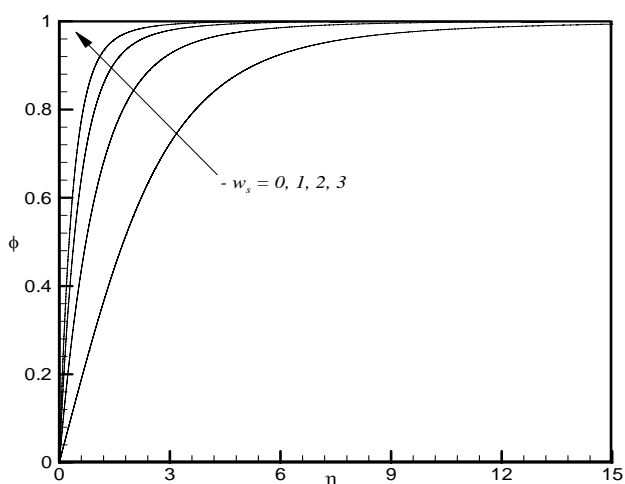

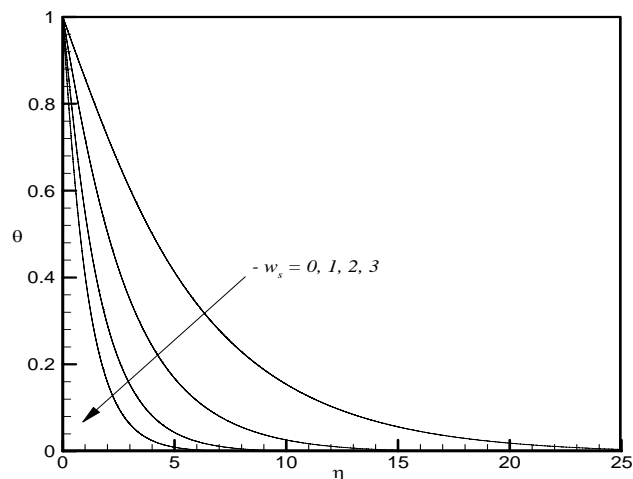Fig. 4 (b)Temperature variation for different values of w_s

The effect of the slip parameter ε on the nondimensional concentration and temperature profiles are presented in Figs. 5 (a)-(b) respectively keeping all other parameters values fixed. The case $\varepsilon = 0$ corresponds to no-slip at the surface of the disk. From Fig. 5 (a) it is found that concentration of the particles within the boundary layer decreases with the increase of the slip parameter. For large values of ε i.e. $\varepsilon \to \infty$ (full slip), the rotating disk has no effect on the fluid motion. Because in this range of ε the flow becomes entirely potential, therefore, there will be no motion in the fluid. This can be further explained as follows: the centrifugal force acting on the rotating disk will throw out the fluid that sticks to it. On the other hand the flow in the axial direction will come forward to compensate this thrown fluid. But increasing the slip on the surface of the disk reduces the amount of fluid that can stick on it; as a consequence the efficiency of the rotating disk is reduced substantially and is unable to transfer its circumferential momentum to the fluid particles. A reduction in the circumferential velocity results in a reduction in the centrifugal force which in turn decreases the inward axial velocity as a consequence the concentration of the fluid particles decreases. This result is consistent with the work of [33] even in the presence of thermophoresis. On the other hand temperature of the flow field within the boundary layer increases with the increase of the slip parameter as can be seen from Fig. 5 (b).
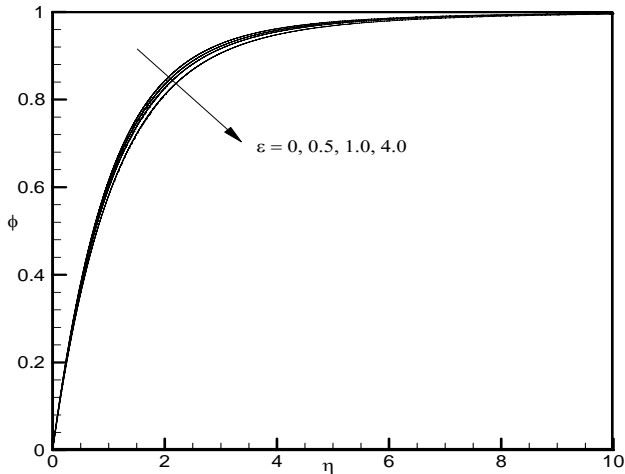

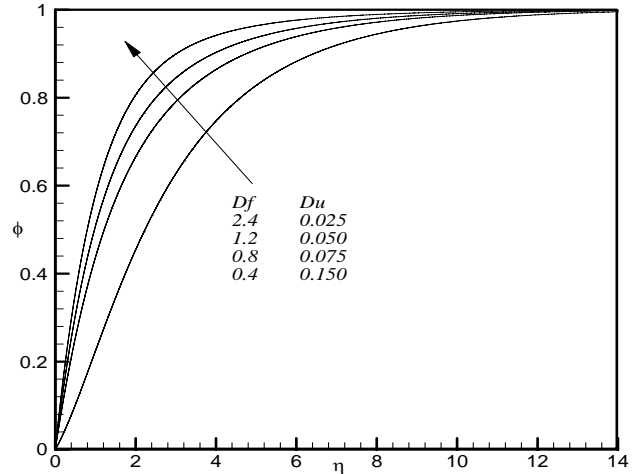Fig. 4 (a) Concentration variation for different values of w_s

World Academy of Science, Engineering and Technology
International Journal of Mathematical and Computational Sciences
Vol:7, No:5, 2013

Fig. 5 (a) Concentration variation for different values of ε

Fig. 5 (b) Temperature variation for different values of ε
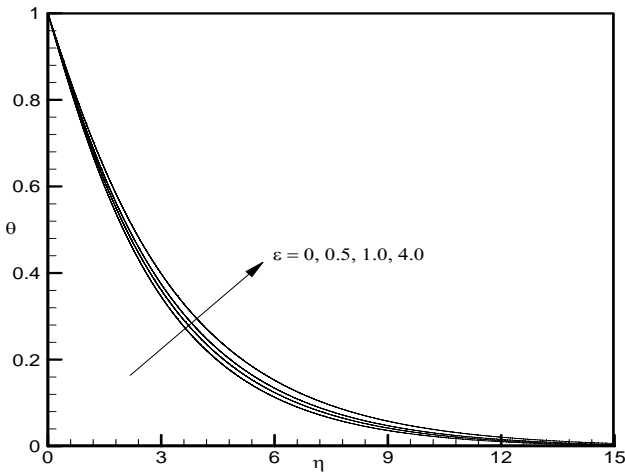

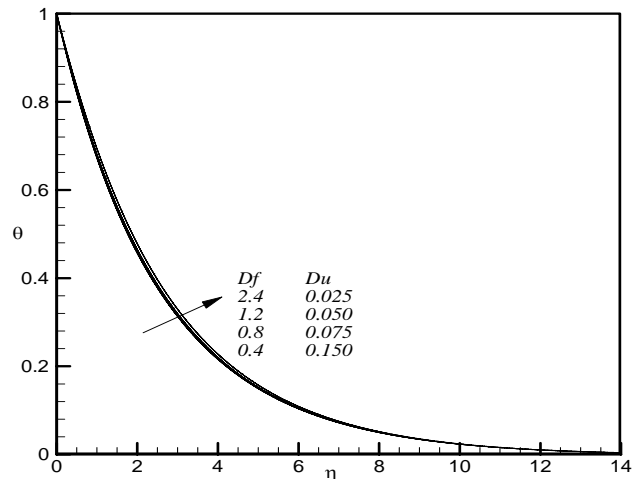Fig. 6 (a) Concentration variation for different values of Df and Du

Fig. 6 (b) Temperature variation for different values of Df and Du

The effects of the thermal-diffusion and diffusion-thermo parameters on the concentration and temperature profiles within the boundary layer are depicted in Figs. 6 (a)-(b), respectively. It can be seen from Fig. 6 (a) that concentration of the fluid particles increases quite rapidly with the combined effects of Df and Du. We observe that quantitatively at $\eta = 3$ and Df decreases from 2.4 to 1.2 (or Du increases from 0.025 to 0.050) there is approximately 21% increase in the concentration value, whereas the corresponding increase is approximately 6% when Df decreases from 1.2 to 0.8 (or Du increased from 0.05 to 0.075) and 5.5% when Df decrease from 0.8 to 0.4 respectively (or Du increased from 0.075 to 0.15). The temperature of the fluid within the boundary layer is also increases with the combined effects of Soret and Dufour effects.

In Figs. 7 (a)-(b) we have presented concentration and temperature profiles for some representative values of the temperature parameter $N_t = 0$, 0.4, 0.6, 0.8, 0.99 to examine the effect of thermophoresis on the particle deposition onto a rotating disk. Fig. 7 (a) shows that concentration of the fluid particles within the boundary layer decreases with the increase of the values of N_t. Fig. 7 (b) shows that temperature of the fluid within the boundary layer decreases with the increase of the temperature parameter. This is due to the fact that an increase in N_t decreases the disk's surface temperature (T_w) as a consequence temperature within the boundary layer decreases.

Figs. 8 (a)-(b) show the spatial concentration evolution of particles within the boundary layer for various values of the Schmidt number Sc. The values of Schmidt number are taken for hydrogen ($Sc = 0.22$), helium ($Sc = 0.30$), water-

World Academy of Science, Engineering and Technology
International Journal of Mathematical and Computational Sciences
Vol:7, No:5, 2013

vapor ($Sc = 0.62$) and carbon-dioxide ($Sc = 0.94$). As the Schmidt number increases, the concentration boundary layer becomes thinner. Fig. 8 (a) plotted for small values of Sc, reveals that concentration profiles increase with Schmidt number. Fig. 8 (b) plotted for large values of Sc, shows that increase of these profiles is very steep for large Schmidt numbers close to the wall. From the physical point of view, for smaller values of the Schmidt number, Brownian diffusion effect is more important as compared to the convection effect. However, for large values of Sc, the diffusion effect is minimal as compared to the convection effect and, therefore, effect of thermophoresis alters the concentration boundary layer significantly. This finding well agrees with the similar conclusion made by [37].
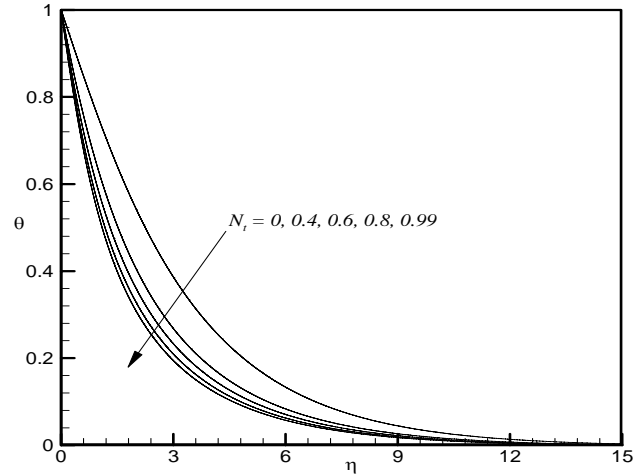

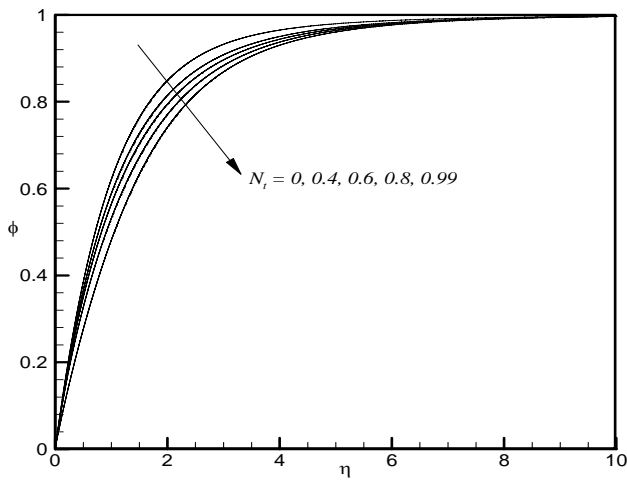Fig. 7 (b) Temperature variation for different values of N_t

Fig. 7 (a) Concentration variation for different values of N_t

TABLE IV

VARIATIONS OF LOCAL STANTON NUMBER ($St_r Sc \, \mathrm{Re}_r^{1/2}$) AND THERMOPHORETIC VELOCITY (W_T^*) FOR DIFFERENT VALUES OF THE PERTINENT PARAMETERS

Ha	R	w_s	ε	N_t	κ	Du	Df	$St_r Sc \, \mathrm{Re}_r^{1/2}$	W_T^*
0.0	1.0	-1.0	0.2	0.1	0.5	0.3	0.2	0.017823	0.982481
0.5								0.017089	0.960688
1.0								0.016089	0.927955
1.5								0.015600	0.905692
0.5	0.1	-1.0	0.2	0.1	0.5	0.3	0.2	0.006801	1.003052
	1.0							0.017089	0.960688
	10							0.029810	0.918131
	100							0.032343	0.909835
0.5	1.0	0.0	0.2	0.1	0.5	0.3	0.2	0.009737	0.323160
		-0.5						0.012979	0.603300
		-1.0						0.017429	0.961357
		-2.0						0.023216	1.367184
0.5	1.0	-1.0	0.0	0.1	0.5	0.3	0.2	0.017221	0.959950
			0.5					0.016700	0.948596
			1.0					0.016214	0.931133
			4.0					0.015407	0.900137
0.5	1.0	-1.0	0.2	0.0	0.5	0.3	0.2	0.000000	0.968452
				0.4				0.155395	0.934183
				0.6				0.413015	0.921097
				0.8				1.176592	0.917839
0.5	1.0	-1.0	0.2	0.1	0.0	0.3	0.2	0.000000	0.959905
					0.4			0.013672	0.960532
					0.8			0.027339	0.961157
					1.2			0.041001	0.961781

World Academy of Science, Engineering and Technology
International Journal of Mathematical and Computational Sciences
Vol:7, No:5, 2013

0.5	1.0	-1.0	0.2	0.1	0.5	0.0	0.2	0.022672	0.942154
						0.3		0.017089	0.960688
						0.6		0.011277	0.979980
						1.0		0.003148	1.006969
0.5	1.0	-1.0	0.2	0.1	0.5	0.3	0.0	0.016771	1.013321
							0.2	0.017089	0.960688
							0.1	0.016929	0.987265
							0.06	0.016865	0.997749

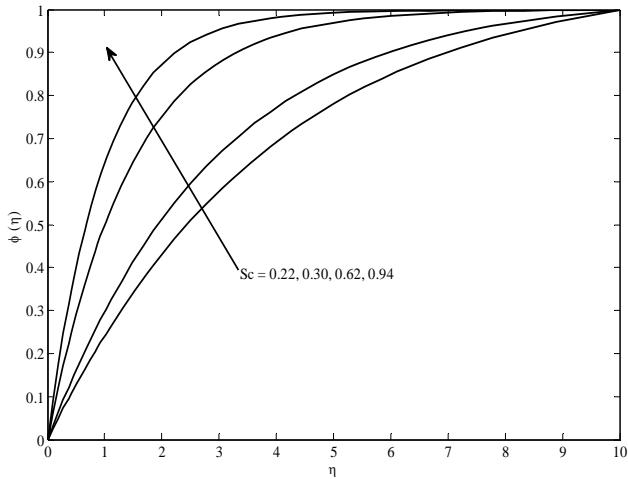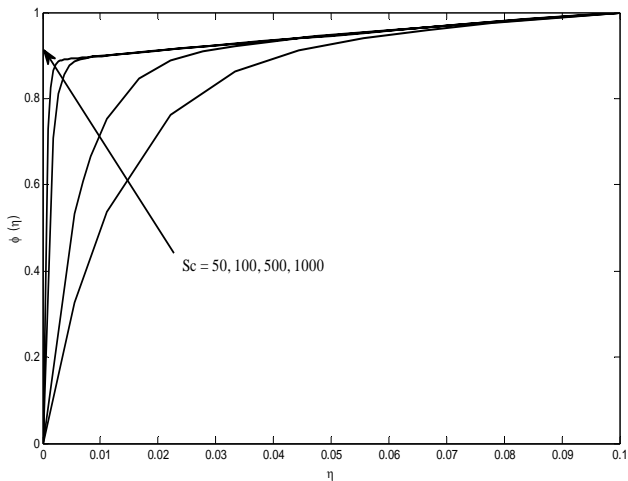Fig. 8 (a) Concentration variation for different values of Sc (< 1)
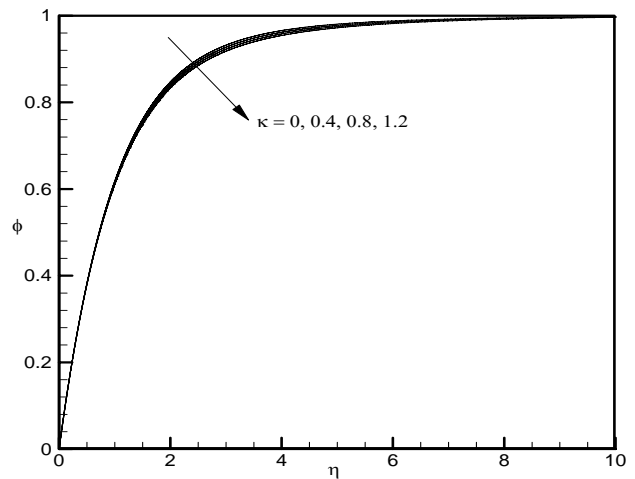

Fig. 9 Concentration variation for different values of κ

Fig. 8 (b) Concentration variation for different values of Sc $(>> 1)$

In Fig. 9, the effect of the thermophoretic coefficient κ on the concentration profile across the boundary layer is depicted. For the parametric conditions used in Fig. 9, the effect of increasing the thermophoretic coefficient κ is to increase the slope of the concentration profiles except very close to the surface of the disk ($\eta < 0.7$), where these profiles decrease with the increase of κ. This is due to the fact that thermophoresis plays a suction-like effect on particles for a cold surface.

Table IV shows the variations of local Stanton number (or inward axial nondimensional thermophoretic deposition velocity) and nondimensional thermophoretic velocity (W_T^*) for different values of the pertinent parameters. This table shows that deposition flux and inward axial thermophoretic deposition velocity increases with the increase of the suction parameter w_s, thermophoretic parameter κ and the diffusion-thermo parameter Du. Table IV further reveals that local Stanton number decreases with the increase of the Hartmann number Ha, radiation parameter R, slip parameter ε, temperature parameter N_t, and the thermal-diffusion parameter Df.

Table IV also reveals that nondimensional thermophoretic velocity (W_T^*) increases with the increase of the radiation parameter, suction parameter, temperature parameter, thermophoretic parameter whereas it decreases with the increase of the Hartmann number, slip parameter, and the diffusion-thermo parameter.

World Academy of Science, Engineering and Technology
International Journal of Mathematical and Computational Sciences
Vol:7, No:5, 2013

VI. Conclusions

Thermophoretic deposition of nanoparticles due to the three dimensional steady forced convective laminar flow of a viscous incompressible fluid over a rapidly rotating porous disk in the presence of partial slip at its surface under the action of an applied magnetic field has been analyzed. The thermal-diffusion and diffusion-thermo effects on the particle deposition mechanism are also taken into account together with the effect of thermal radiation. The governing nonlinear partial differential equations such as continuity, momentum, energy and concentration are transformed into nonlinear ordinary differential equations using similarity analysis, and the solutions are obtained through the very efficient computer algebra software MATLAB. Results for the dimensionless concentration and temperature profiles are displayed graphically delineating the effect of various parameters characterizing the flow. Thermophoretic velocity and the thermophoretic deposition flux of particles within the boundary layer are also tabulated for various values of the pertinent parameters. From the present investigation the following conclusions may be drawn

i. Particles concentration within the boundary layer decreases with the increase of the Hartmann number, Radiation parameter, slip parameter, temperature parameter and the thermophoretic parameter whereas it increases with the increase of the suction parameter.

i. Temperature of the particles across the boundary layer decreases with the increase of the radiation parameter, suction parameter and the temperature parameter whereas it increases with the increase of the Hartmann number, and the slip parameter.

i. Combined effects of thermal-diffusion and diffusion-thermo leads to the increase of the particles concentration as well as their temperature within the boundary layer.

r. Thermophoretic deposition flux of particles increases with the increase of the suction parameter w_s, thermophoretic parameter κ and the Dufour number Du whereas it decreases with the increase of the Hartmann number Ha, radiation parameter R, slip parameter ε, temperature parameter N_t, and the thermal-diffusion parameter Df.

r. Thermophoretic velocity of the particles across the boundary layer increases with the increase of the radiation parameter, suction parameter, temperature parameter, thermophoretic parameter whereas it decreases with the increase of the Hartmann number, slip parameter, and the Diffusion-thermo parameter.

vi. For smaller values of the Schmidt number, Brownian diffusion effect is found more important than the convection effect.

vii. For large values of Sc, the diffusion effect is found minimal as compared to the convection effect.

References

[1] S.L. Goren, "Thermophoresis of aerosol particles in laminar boundary layer on flat plate,"*J. Colloid Interface Sci.*, vol. 61, pp. 77-85, 1977.
[2] L. Talbot, R.K. Cheng, R.W. Schefer, D.R. Wills, "Thermophoresis of particles in a heated boundary layer,"*J. Fluid Mech.*, vol. 101, pp. 737-758, 1980.
[3] G.M. Homsy, F.T. Geyling, K.L. Walker, "Blasius series for thermophoresis deposition of small particles,"*J. Colloid Interface Sci.*, vol. 83, pp. 495-501, 1981.
[4] A.F. Mills, X. Hang, F. Ayazi, "The effect of wall suction and thermophoresis on aerosol-particle deposition from a laminar boundary layer on a flat plate," *Int. J. Heat Mass Transfer*, vol.27, pp. 1110-1114, 1984.
[5] M. Epstein, G.M. Hauser, R.E. Henry, "Thermophoretic deposition of particles in natural convection flow from a vertical plate,"*J. Heat Transfer*, vol.107, pp. 272-276, 1985.
[6] G.K. Batchelor, C. Shen, "Thermophoretic deposition of particles in gas flowing over cold surface," *J. Colloid Interface Sci.*, vol.107, pp. 21-37, 1985.
[7] W.W. Nazaroff, G.R. Cass, "Particle deposition from a natural convection flow onto a vertical isothermal flat plate," *J. Aerosol Sci.*, vol.18, pp.445-455, 1987.
[8] G. Jia, J.W. Cipolla, Y. Yener, "Thermophoresis of a radiating aerosol in laminar boundary layer flow,"*J. Thermophys. Heat Transfer*, vol. 6, pp. 476-482, 1992.
[9] M.C. Chiou, J.W. Cleaver, "Effect of thermophoresis on submicron particle deposition from a laminar forced convection boundary layer flow on to an isothermal cylinder,"*J. Aerosol Sci.*, vol. 27, pp. 1155-1167, 1996.
[10] S. Jayaraj, K.K. Dinesh, K.L. Pallai, "Thermophoresis in natural convection with variable properties,"*Heat Mass Transfer*, vol.34, pp. 469-475, 1999.
[11] R. Tsai, "A simple approach for evaluating the effect of wall suction and thermophoresis on aerosol particle deposition from a laminar flow over a flat plate,"*Int. Commun. Heat Mass Transfer*, vol. 26, pp. 249-257, 1999.
[12] Y.P. Chang, R. Tsai, F.M. Sui, "The effect of thermophoresis on particle deposition from a mixed convection flow onto a vertical flat plate," *J. Aerosol Sci., vol.* 30, pp. 1363-1378, 1999.
[13] A.J. Chamkha, I. Pop, "Effect of thermophoresis particle deposition in free convection boundary layer from a vertical flat plate embedded in a porous medium,"*Int. Commun. Heat Mass Transfer*, vol.31, pp. 421-430, 2004.
[14] A.J. Chamkha, A.F. Al-Mudhaf, I. Pop, "Effect of heat generation or absorption on thermophoretic free convection boundary layer from a vertical flat plate embedded in a porous medium,"*Int. Commun. Heat Mass Transfer*, vol.33, pp. 1096-1102, 2006.
[15] M.A. Seddeek, 'Influence of viscous dissipation and thermophoresis on Darcy–Forchheimer mixed convection in a fluid saturated porous media,"*J. Colloid Interface Sci.*, vol. 293, pp. 137-142, 2006.
[16] A. Postelnicu, "Effects of thermophoresis particle deposition in free convection boundary layer from a horizontal flat plate embedded in a porous medium,"*Int. J. Heat Mass Transfer*, vol. 50, pp. 2981-2985, 2007.
[17] M.S. Alam, M.M. Rahman, M.A. Sattar, "Effects of variable suction and thermophoresis on steady MHD combined free-forced convective heat and mass transfer flow over a semi-infinite permeable inclined plate in the presence of thermal radiation,"*Int. J. Thermal Sci.*, vol.47, pp. 758-765, 2008.
[18] M.S. Alam, M.M. Rahman, M.A. Sattar, "Effects of chemical reaction, thermophoresis and heat generation/absorption on steady MHD mixed convective heat and mass transfer flow along a semi-infinite inclined porous flat plate with viscous dissipation and joule heating,"*Canadian J. Phys.*, vol.86, pp.1057-1066, 2008.
[19] M.S. Alam, M.M. Rahman, M.A. Sattar, "On the effectiveness of viscous dissipation and Joule heating on steady Magnetohydrodynamic heat and mass transfer flow over an inclined radiate isothermal permeable surface

World Academy of Science, Engineering and Technology
International Journal of Mathematical and Computational Sciences
Vol:7, No:5, 2013

in the presence of thermophoresis,"*Commun. Nonlinear. Sci. Numer. Simulat*,vol. 14, pp. 2132-2143, 2009.

[20] M.S. Alam, M.M. Rahman, M.A. Sattar,"Transient magnetohydrodynamic free convective heat and mass transfer flow with thermophoresis past a radiate inclined permeable plate in the presence of variable chemical reaction and temperature dependent viscosity,"*Nonlin. Analy. Model. Control*,vol.14, pp. 3–20, 2009.

[21] N.F.M. Noor, S. Abbasbandy, I. Hashim, "Heat and mass transfer of thermophoretic MHD flow over an inclined radiate isothermal permeable surface in the presence of heat source/sink,"*Int. J. Heat Mass Transfer*,vol. 55, pp. 2122-2128, 2012.

[22] A. Postelnicu, "Thermophoresis particle deposition in natural convection over inclined surfaces in porous media,"*Int. J. Heat Mass Transfer*, vol. 55, pp. 2087-2094, 2012.

[23] T.von Karman, "Uberlaminare und turbulentereibung,"*ZAMM*,.vol.1, pp.233-255, 1921.

[24] N. Kelson, A. Desseaux, "Note on porous rotating disk flow", *ANZIAM J.*, vol.42(E), pp. C837-C855, 2000.

[25] H.I. Andersson, E. de Korte, "MHD flow of a power law fluid over a rotating disk,"*European J. Mech. B. Fluids*, vol.21, pp. 317-324, 2002.

[26] H.S. Takhar, A.K. Singh, G. Nath, "Unsteady MHD flow and heat transfer on a rotating disk in an ambient fluid,"*Int. J. Therm. Sci.*, vol.41, pp.147-155, 2002.

[27] M. Miklavcic, C.Y. Wang, "The flow due to a rough rotating disk", *Z. Angew. Math. Phys.*, vol.55,pp. 235-246, 2004.

[28] K.A. Maleque, M.A. Sattar, "Steady laminar convective flow with variable properties due to a porous rotating disk,"*J. Heat Trans.*, vol.127, pp.1406-1409, 2005.

[29] K.A. Maleque, M.A. Sattar, "The effects of variable properties and Hall current on steady MHD laminar convective fluid flow due to a porous rotating disk,"*Int. J. Heat Mass Transfer*, vol.48, pp. 4963-4972, 2005.

[30] A. Arikoglu, I. Ozkol, "On the MHD and slip flow over a rotating disk with heat transfer,"*Int. J. Numer Methods Heat Fluid Flow*,vol.28, pp.172-184, 2006.

[31] E. Osalusi, P. Sibanda, "On variable laminar convective flow properties due to a porous rotating disk in a magnetic field,"*Romanian J. Phys.*, vol.51, pp. 933-944, 2006.

[32] E. Osalusi, J. Side, R. Harris, "Thermal-diffusion and diffusion-thermo effects on combined heat and mass transfer of a steady MHD convective and slip flow due to a rotating disk with viscous dissipation and Ohmic heating,"*Int. Commu. Heat Mass Transfer*,vol.35, pp.908-915, 2008.

[33] M.M. Rahman, "Convective hydromagnetic slip flow with variable properties due to a porous rotating disk,"*SQU J. Sci.*,vol.15, pp. 55-79, 2010.

[34] C.-G. Song, J. Hwang, "Particle deposition on a rotating disk in application to vapor axial deposition (VAD) process,"*J. Aerosol Sci.*, vol. 29, pp. 99-114, 1998.

[35] C.C. Wang, "Combined effects of inertia and thermophoresis on particle deposition onto a wafer with wavy surface,"*Int. J. Heat Mass Transfer,*vol.49, pp.1395-1402, 2006.

[36] C.L. Chen, K.C. Chan, "Combined effects of thermophoresis and electrophoresis on particle deposition onto a wavy surface disk,"*Int. J. Heat Mass Transfer*,vol.51, pp. 2657-2664, 2008.

[37] M.M. Rahman, A. Postelnicu, "Effects of thermophoresis on the forced convective laminar flow of a viscous incompressible fluid over a rotating disk,"*Mech. Res. Commun.*,vol. 37, pp. 598–603, 2010.

[38] M. Gad-el-Hak, "The fluid mechanics of microdevices–the freeman scholar lecture,"*J. Fluids Eng.*, vol. 121, pp. 5–33, 1999.

[39] J.-S. Lin, C.J. Tsai, C.P. Chang, "Suppression of particle deposition in tube flow by thermophoresis,"*Aerosol Sci.*, vol. 35, pp. 1235–1250, 2004.

[40] M.M. Rahman, M.A. Lawatia, I.A. Eltayeb, N. Al-Salti, "Hydromagnetic slip flow of water based nanofluids past a wedge with convective surface in the presence of heat generation (or) absorption,"*Int. J. Thermal Sci.*, vol. 57, pp.172-182, 2012.

M. M. Rahman wasborn in Pabna, Bangladesh on 7th January 1973. He obtained B.Sc. (Hons) in Mathematics and M.Sc. in Applied Mathematics from the Department of Mathematics, University of Dhaka, Bangladesh. For his outstanding results in B.Sc. (Hons) and M.Sc. examinations, he was awarded Raja Kalinarayan Scholarship (one of the most prestigious scholarships of the Dhaka University) and AshaLataSenGold Medal, respectively. He got his Ph.D. in Applied Mathematics from the Department of Mathematics, University of Glasgow, United Kingdom in 2003 under the direction of Professor David R Fearn, FRSE. His research interests include magnetohydrodynamics, mathematical fluid mechanics, nano-fluidic phenomena, heat and mass transfer, non-Newtonian fluids, transport in porous media, and bio-fluid flows.

Dr. Rahman is an Associate Professor in the Department of Mathematics and Statistics, Sultan Qaboos University, Sultanate of Oman. Before joining Sultan Qaboos University, he worked in the Department of Mathematics, University of Dhaka, Bangladesh. He has authored/co-authored a total of 69research papers.

Dr. Rahman is a life member of Bangladesh Mathematical Society and Mathematics Alumni, University of Dhaka, Bangladesh.